Available online at www.sciencedirect.com
SCIENCE DIRECT
Journal of Power Sources 147 (2005) 234–240
JOURNAL OF POWER SOURCES
www.elsevier.com/locate/jpowsour

Optimization of reaction condition for solid-state synthesis of $LiFePO_4$-C composite cathodes

S.S. Zhang *, J.L. Allen, K. Xu, T.R. Jow

U.S. Army Research Laboratory, Adelphi, MD 20783-1197, USA

Received 7 December 2004; accepted 4 January 2005
Available online 19 February 2005

Abstract

We optimized synthesis condition of $LiFePO_4$-C composites by solid-state reaction of LiH_2PO_4 and $FeC_2O_4{\cdot}2H_2O$ in the presence of carbon powder. The preparation was conducted under a N_2 flow through two heating steps. First, the starting materials were thoroughly mixed in a stoichiometric ratio and decomposed at 350–380 °C to form the precursor. Second, the resulting precursor was heated at a high temperature to form the crystalline phase $LiFePO_4$. For formation of the precursor, the optimized temperature was 350 °C for $LiFePO_4$ and 380 °C for $LiFePO_4$-C composites, respectively. For formation of crystalline phase composites, the optimized condition was to heat the precursor in a pelletized form at 800 °C for 5 h, and the optimized content of carbon was 3–10 wt.%. In composites, the carbon not only increases the rate capability, but also enhances capacity stability. We found that capacity of the composites increases with specific surface area of carbon. The best result was observed from a composite made of 8.7 wt.% of black pearls BP 2000 having a specific surface area of 1500 $m^2\,g^{-1}$. At room temperature and low current rate (0.02 C), such a composite shows a specific capacity of 159 mAh g^{-1}. Electrochemical properties and cycling performance of the optimized composite also were evaluated.

Keywords: $LiFePO_4$; $LiFePO_4$-C composite; Carbon; Solid-state reaction; Rate capability

1. Introduction

In 1997, Padhi et al. [1] first reported lithium iron phosphate ($LiFePO_4$) as a new cathode material for rechargeable lithium batteries. This material has many advantages compared with conventional cathode materials such as $LiCoO_2$, $LiNiO_2$, and $LiMn_2O_4$, namely, it is environmentally benign, inexpensive, and thermally stable in the charged state [2,3]. In addition, olivine $LiFePO_4$ has a high theoretical capacity of 170 mAh g^{-1}, good cycling stability, and flat discharge potential of 3.4 V versus Li/Li^+. These properties make it an attractive candidate for the cathode material of rechargeable batteries. The main problem with this material is poor rate capability, which is attributed to its low electronic conductivity and slow kinetics of lithium ion diffusion through the $LiFePO_4$–$FePO_4$ interfaces [4,5]. Two approaches have been attempted to overcome this problem. One is to enhance electric conductivity by coating an electron-conducting layer around the particles, such as carbon [6–15], copper [16] and silver [17], or by doping with guest cations [18–20]. The other is to minimize particle size by modifying the synthesis conditions, such as using solution method [21–26] or lowering the sintering temperature [24–28].

The olivine $LiFePO_4$ can be synthesized by the solution method [8,11,14–17,21–26] or by a solid-state reaction method [1,4,9–12,15,18,19,28,29,31]. Most of these methods were carried out through two heating steps of (1) precursor preparation and (2) powder crystallization. Commonly, the final crystallization in these two methods was carried out at high temperature, which requires an inert or reductive atmosphere to prevent oxidization of iron. In the solution method, the precursor is prepared through a chemical reaction in the liquid phase and a subsequent evaporation of the solvent. This process requires additional care to prevent oxidization of the resulting precursor because Fe(II) ions in solution are much

* Corresponding author. Tel.: +1 301 394 0981; fax: +1 301 394 0273.
E-mail address: szhang@arl.army.mil (S.S. Zhang).

0378-7753/$ – see front matter © 2005 Elsevier B.V. All rights reserved.
doi:10.1016/j.jpowsour.2005.01.004

easier to oxidize in air. Therefore, the solution method is less effective although it offers some advantages in making a homogeneous mixture and in reducing particle size. Compared to the solution method, the solid-state reaction offers an easier and more effective approach, which makes it attractive in large-scale synthesis.

Several combinations of the starting materials have been used for the solid-state synthesis of $LiFePO_4$, and it was reported that the optimized temperature for the formation of crystalline phase greatly varied with the starting materials and the method of precursor preparation [26–30]. For example, the optimized temperatures were 550 °C for $Fe(CH_3CO_2)_2$–$NH_4H_2PO_4$–Li_2CO_3 by solid-state reaction [27], 600 °C for $Fe_3(PO_4)_2{\cdot}5H_2O$–Li_3PO_4 by hydrothermal synthesis [30], 700 °C for $Fe_3(PO_4)_2{\cdot}8H_2O$–Li_3PO_4 by solid-state reaction [28], 750 °C for $Fe(NO_3)_3{\cdot}9H_2O$–$(NH_4)_2HPO_4$–$LiNO_3$ by emulsion-drying method [26], and 800 °C for $Fe(CH_3CO_2)_2{\cdot}2H_2O$–$(NH_4)_2HPO_4$–$Li_2CO_3$ in the presence of citric acid by direct solid-state reaction [29]. In addition, it is difficult to find consistent cycling data for the $LiFePO_4$ cathodes because their morphology from different sources varied significantly. On the other hand, it was reported [6,31] that addition of fine carbon to the precursor before the formation of the crystalline phase could reduce the particle size of $LiFePO_4$ and enhance rate capability since the carbon is uniformly dispersed between $LiFePO_4$ grains to form good electronic contacts.

Based on the facts above, we selected $FeC_2O_4{\cdot}2H_2O$ and LiH_2PO_4 as the starting materials for the solid-state synthesis of the $LiFePO_4$-C composites because the oxalates thermally decompose to release reductive CO that may potentially protect Fe(II) from being oxidized. In this work, we optimized the synthesis conditions of the olivine $LiFePO_4$ and its carbon composites by using X-ray diffraction as the structure identification tool and evaluated their electrochemical properties as the cathode of rechargeable lithium batteries.

2. Experimental

$LiFePO_4$ and its carbon composites were prepared by the solid-state reaction of $FeC_2O_4{\cdot}2H_2O$ (99%, Aldrich) and LiH_2PO_4 (99.99+%, Aldrich) without or with addition of carbon as the conducting enhancer. The preparation was conducted through two heating-steps under a N_2 flow to prevent oxidation of iron. A general procedure of the experiment is described as follows. Starting materials were thoroughly mixed in a stoichiometric ratio and heated at 350–380 °C for 5 h in a tubular furnace to form the $LiFePO_4$ precursor. The resulting precursor was reground, pelletized, and heated at high temperature to form the crystalline phase $LiFePO_4$. The temperature and time for the heating were described and discussed in the text. A Perkin-Elmer thermogravimetric analyzer (TGA-7) was used to determine the temperature for the preparation of the $LiFePO_4$ precursor. The crystallographic structure of $LiFePO_4$ was identified by powder X-ray diffraction (XRD) with Cu Kα radiation using a Philips PW 1840 X-ray diffractometer.

For electrochemical testing, a composite electrode with a load of $10 \pm 1\ mg\ cm^{-2}$ was fabricated by a slurry coating method. Using *N*-methylpyrrolidone as the solvent, a slurry of 75% $LiFePO_4$, 20% carbon black, and 5% poly(acrylonitrile-co-methyl methacrylate) was prepared and coated onto an aluminum foil. For $LiFePO_4$-C composite, the amount of carbon black was adjusted so that the total content of carbon was 20%. The electrode film was cut into small discs with an area of 1.27 cm^2 and dried at 120 °C for 8 h under vacuum before use. In an Ar-filled glove-box, Li/$LiFePO_4$ button cells were assembled using Celgard® 3500 membrane as the separator and a 1.2 M $LiPF_6$ solution in a 3:3:4 (wt.) mixture of propylene carbonate, ethylene carbonate and ethylmethyl carbonate as the electrolyte. A Tenney Environmental Oven Series 942 was used as a constant temperature provider for the test. A cyclic voltammetry test was performed on an EG&G PAR potentiostat/galvanostat model 273A controlled by a personal computer. A cycling test was performed using a Maccor Series 4000 tester. Unless noted otherwise, the cell was cycled by charging at 0.2 C to 4.2 V and holding it at 4.2 V for 10 h or until the current declined to 0.05 C, and discharging at 0.2 C to 2.0 V. The C rate was calculated from the weight and theoretical capacity of $LiFePO_4$.

3. Results and discussion

3.1. Preparation of $LiFePO_4$ precursor

Thermal gravimetry (TG) was used to determine the temperature for the preparation of precursor. Fig. 1 displays TG traces of the starting materials and their mixture, which were recorded at a scanning rate of 10 °C min^{-1} under N_2 flow. According to the change of weight percentage, the following results are obtained:

(1) For $FeC_2O_4{\cdot}2H_2O$, it first lost 2 moles of H_2O at ~156 °C, and then decomposed into FeO from 320 to 450 °C.

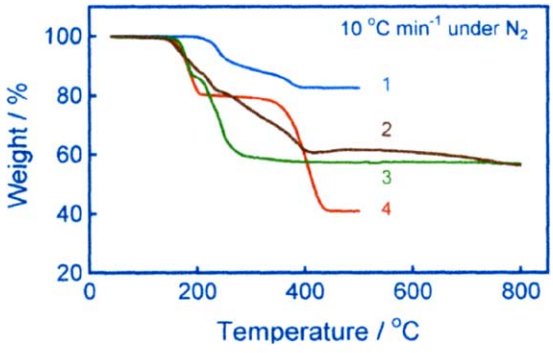

Fig. 1. Thermal gravimetry traces of the starting materials. (1) $FeC_2O_4{\cdot}2H_2O$, (2) LiH_2PO_4, (3) 1:1 (mol) $FeC_2O_4{\cdot}2H_2O$–LiH_2PO_4 mixture, and (4) sample 3 with addition of 5 wt.% carbon black.

(2) For LiH_2PO_4, it lost a 0.5 mole of H_2O at ~200 °C to form a dimer ($Li_2H_2P_2O_7$), which further lost 1 mole of H_2O between 255 and 400 °C to form $Li_2P_2O_6$.
(3) For $FeC_2O_4{\cdot}2H_2O$–LiH_2PO_4 mixture, it first lost H_2O of $FeC_2O_4{\cdot}2H_2O$ at ~156 °C, and formed $LiFePO_4$ precursor between 200 and 300 °C. Above 350 °C, the weight almost remained constant, indicating that the precursor had the same chemistry as $LiFePO_4$.
(4) The same mixture, with addition of carbon black, lost H_2O at the same temperature (156 °C). However, temperature range for the formation of precursor was significantly extended (200–410 °C) and the resulting precursor kept a very slow weight-loss until the experiment ended. The latter behavior is likely associated with burning of carbon by a small amount of oxygen included in the N_2 flow.

To confirm TG results, we performed XRD analysis on the starting materials and the resulting precursor, as shown in Fig. 2. Comparing XRD patterns of the starting materials and precursor, we see that nearly all diffraction peaks in the starting materials vanish from the precursor, and that the precursor only has a couple of small and wide diffraction peaks. These observations indicate that after heating at 350 °C for 5 h, the starting materials were completely decomposed, and the formed precursor could be amorphous or slightly crystalline. Based on the results of TG and XRD, the optimized temperature for the preparation of $LiFePO_4$ and $LiFePO_4$-C precursors was at 350 and 380 °C, respectively.

3.2. Optimized temperature for formation of crystalline $LiFePO_4$

Two procedures were used to evaluate the effect of the heating temperature on the capacity of the $LiFePO_4$ cathode. For this purpose, a fixed time of 10 h was adopted for these two procedures. One was that the precursor powder was directly heated without being pelletized, and the other was that the precursor powder was first pelletized under a pressure of 3200 kg cm^{-2} and then heated. Fig. 3 compares the capacity of the $LiFePO_4$ cathodes made by these two procedures. It is shown that the cathodes made by the first procedure have inferior capacity to those by the second method. A similar result has also been reported elsewhere [31], which was attributed to the formation of an impurity $Fe_3(PO_4)_2$ phase due to insufficient mixing of the reactants. In the first procedure, the $Fe_3(PO_4)_2$ impurities are possibly present although there are no visible $Fe_3(PO_4)_2$ diffraction peaks in XRD patterns of the samples. This is because XRD cannot detect the impurity at levels below 5% [7], or because the impurity grains are too small to be detected. In the second procedure, the pelletization promotes better contact between the reactants, which makes the formation of $LiFePO_4$ more complete. Therefore, the $LiFePO_4$ such-made has a higher capacity. As shown in Fig. 3, the optimized temperature for both procedures was 800 °C, and the highest capacity was 107 mAh g^{-1} for the one prepared by the second procedure. The capacity of the $LiFePO_4$ was decreased as the temperature was higher or lower than 800 °C. This is because high temperature induces growth and aggregation of $LiFePO_4$ particles [24–27,31], and meanwhile it enhances the reducing ability of carbon so that Fe and P are reduced in parallel to form undesirable Fe_2P impurities [32]. Whereas low temperature causes the crystallization process to be incomplete, and also induces formation of trivalent iron impurities due to oxidization of Fe(II) by the small amount of oxygen included in the N_2 flow [27].

Fig. 4 shows XRD patterns of the $LiFePO_4$ powders made by the second procedure at different temperatures. All diffraction peaks can be attributed to an ordered olivine $LiFePO_4$ structure, and no other peaks relating to a second phase are observed throughout the temperature range. The peaks gradually sharpen with increasing temperature, which indicates an increase of crystallinity as may occur from growth of grain size, ordering of local structure, and release of lattice strain.

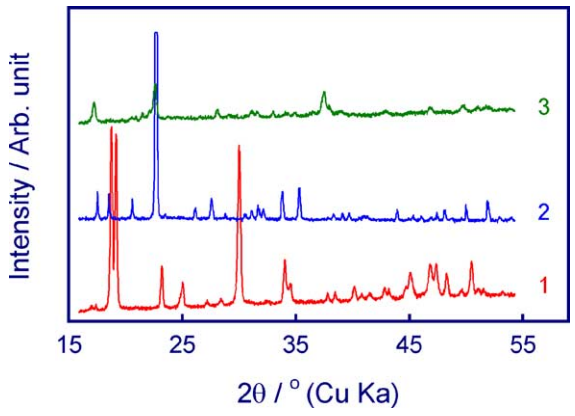

Fig. 2. XRD patterns of the starting materials and precursor. (1) $FeC_2O_4{\cdot}2H_2O$, (2) LiH_2PO_4, (3) precursor formed after heating a 1:1 (mol) $FeC_2O_4{\cdot}2H_2O$-LiH_2PO_4 mixture at 350 °C for 5 h.

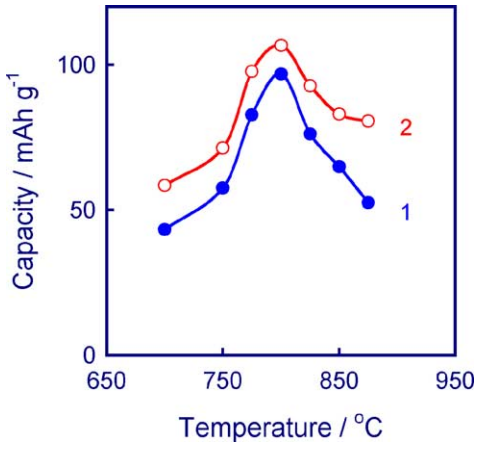

Fig. 3. Effect of heating temperature on the capacity of $LiFePO_4$ cathodes prepared by different procedures. (1) by heating precursor powder, (2) by heating pelletized precursor.

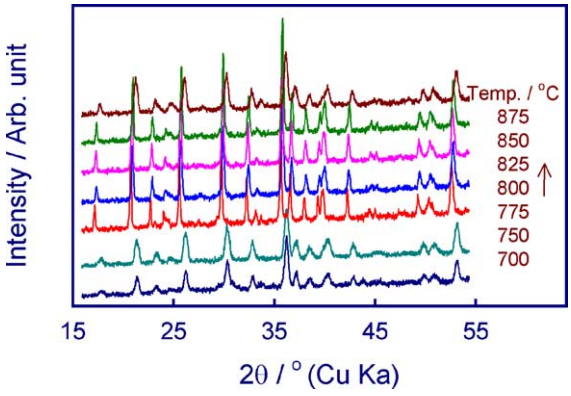

Fig. 4. XRD patterns of $LiFePO_4$ powders prepared at different temperatures.

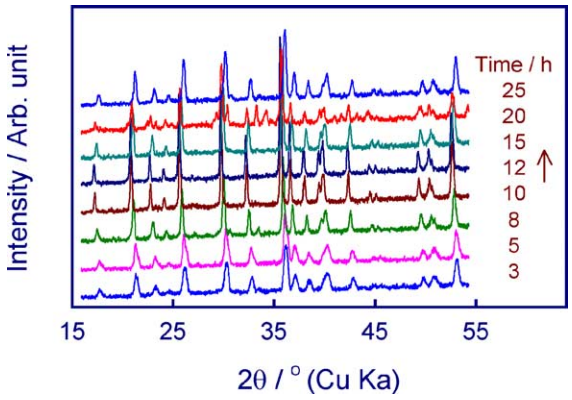

Fig. 5. XRD patterns of the 95:5 $LiFePO_4$-C composites prepared by heating precursor at 800 °C for different times.

It appears that the relationship between heating temperature and capacity, as shown in Fig. 3, is associated with the effect of crystallinity of $LiFePO_4$ cathodes.

3.3. Optimized time for formation of crystalline phase composites

TG analysis has shown that formation of $LiFePO_4$ and $LiFePO_4$-C composites occurs in different temperature ranges. Because $LiFePO_4$-C composites are preferable in practical applications, we chose a 95:5 $LiFePO_4$-C composite as the sample to optimize the heating time. In this experiment, a large amount of precursor was prepared by heating the mixture of starting materials and carbon black at 380 °C for 5 h. The resulting precursor was reground, split equally into eight portions, and then pelletized under a pressure of 3200 kg cm^{-2}. The pellets were individually heated at 800 °C for different times. In addition to enhancing electronic conductivity of the composites, carbon also offers many other advantages, such as, (1) at high temperature, it provides a reducting environment to prevent oxidation of iron, (2) its presence suppresses growth of grain size [6,9], and (3) it serves as a lubricant for the milling process, therefore, no liquid carrier is necessary for the mixing process by ball-milling.

Fig. 5 displays XRD patterns of the composites made by heating the precursor for different times. All diffraction peaks belong to the olivine $LiFePO_4$ phase as carbon black used in this experiment is amorphous and it did not generate any diffraction peaks. It can be seen that, with increasing of the heating time, the peaks rapidly sharpen from 3 to 12 h, and then remain unchanged from 12 to 25 h. This observation indicates that growth of the crystalline phase mainly takes place in the initial 10 h, the crystallinity no longer increases for the further extended period. This behavior could be attributed to the effect of carbon reducing the size of $LiFePO_4$ grains [6,9].

A plot of capacity versus heating time exhibits a strong effect of the heating time on the capacity of composites (Fig. 6). The capacity of the composites varies significantly between 3 and 10 h, and it remains nearly constant 80–85 mAh g^{-1} for longer times. This observation is in good agreement with the XRD results. It is shown in Fig. 6 that a maximum capacity of 118 mAh g^{-1} was achieved when the heating time was 5 h.

3.4. Effect of the carbon content on performance of $LiFePO_4$-C composite

Using the temperature and time optimized above, we prepared a series of composites with carbon content ranging from 0 to 17% and evaluated the effect of carbon content on the capacity. Fig. 7 illustrates the correlation of carbon content and capacity. The capacity initially increases with carbon content, remains maximum in the range from 3.5 to 10.3%, and rapidly decreases with further increase in the carbon content. Thus, optimized capacities of 118–126 mAh g^{-1} were obtained as the range of carbon content was in 3.5–10.3%. Initial increase of the capacity can be easily explained in terms of enhanced electronic conductivity due to the use of conducting carbon. However, it is somewhat surprising to find a rapid decrease as the carbon content exceeds 10.3%. To understand this observation, we ran XDR on the samples, and plotted XRD patterns in Fig. 8. Diffraction peaks gradually widen with increasing carbon content, which implies a decrease in crystallinity of the composites. Possible reasons for this fact are (1) amorphous carbon phase dilutes the density of

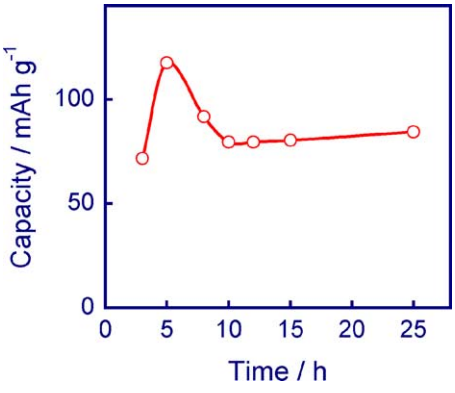

Fig. 6. Effect of heating time on the capacity of the 95:5 $LiFePO_4$-C composites prepared by heating precursor at 800 °C.

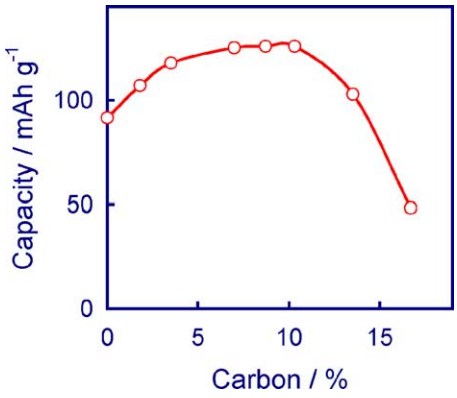

Fig. 7. Effect of carbon content on the capacity of the $LiFePO_4$-C composites prepared by heating precursor at 800 °C for 5 h.

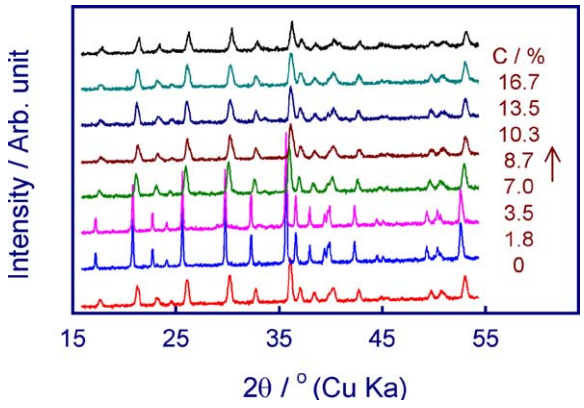

Fig. 8. XRD patterns of the $LiFePO_4$-C composites with different carbon contents.

the crystalline $LiFePO_4$ phase, (2) excess carbon suppresses formation of crystalline $LiFePO_4$ phase, and (3) high carbon content combined with high temperature (800 °C) reduces Fe and P to form inactive Fe_2P [32].

3.5. Effect of the type of carbons on capacity of $LiFePO_4$-C composite

Four types of carbons with different specific surface areas were adopted to synthesize 95:5 $LiFePO_4$-C composites by heating the precursor at 800 °C for 5 h. Table 1 summarizes the relationship between physical properties of carbons and capacity of their composites. Table 1 shows that capacity of the composites has no obvious correlation with the particle size and density of carbon. However, the capacity

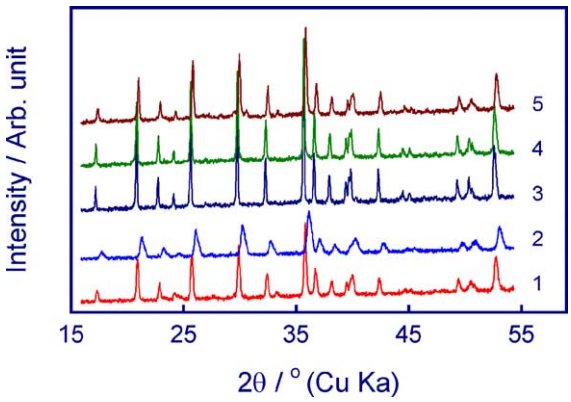

Fig. 9. XRD patterns of the 95:5 $LiFePO_4$-C composites with different types of carbons, which were prepared by heating precursor at 800 °C for 5 h.

increases with specific surface area of carbon. The composite with black pearls 2000, having a specific surface area of 1500 $m^2\,g^{-1}$, shows the highest capacity of 132 mAh g^{-1}. Fig. 9 compares XRD patterns of these composites with different carbons. It is indicated that the composites with high surface carbon (patterns 3 and 4) present sharper diffraction peaks, while the one with low surface carbon (patterns 2 and 5) generate wider diffraction peaks. The latter are very similar to those observed from $LiFePO_4$ (see pattern 1). Based on these results, we recommend the carbon having a high surface area for the preparation of $LiFePO_4$-C composites.

3.6. Evaluation on electrochemical properties of the optimized composite

Electrochemical properties of the $LiFePO_4$-C composite made by using 5% black pearls 2000 and optimized conditions were evaluated. Cyclic voltammograms of the lithium cells with $LiFePO_4$ and $LiFePO_4$-C composite, respectively, are shown in Fig. 10. It is estimated that both cells have a similar coulombic efficiency of 95–97%. However, the cell with $LiFePO_4$-C composite exhibits much sharper current peaks and delivers higher capacity (131 mAh g^{-1}) than the control cell (112 mAh g^{-1}), indicating that the composite has an improved electrochemical kinetics due to the enhanced electronic conductivity between active cathode grains by carbon.

Fig. 11 compares discharging curves of the Li/$LiFePO_4$-C cell at different temperatures. We see that near room temperatures (<30 °C), the temperature strongly affects the capacity of the cell. At a discharging rate of 0.5 C, the cell could delivery a capacity of 140 mAh g^{-1} at 30 °C, while

Table 1
Physical properties of carbon used in $LiFePO_4$-C composites

Carbon	Supplier	Surface area ($m^2\,g^{-1}$)	Particle size (nm)	Density ($g\,cm^{-3}$)	Fifth capacity (mAh g^{-1})
Graphite SFG6	Timcal	17	6.5	0.07	110
Carbon black	Alfa Aesar	75	42	0.081	110
Printex® XE 2	Dugussa	600	30	0.13	123
Black pearls® 2000	Cabot	1500	12	0.12	132

All data was cited from Suppliers' product brochure.

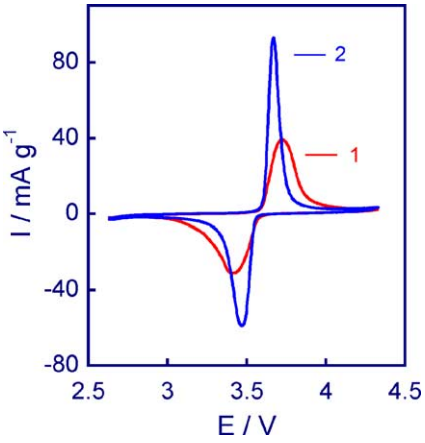

Fig. 10. Cyclic voltammograms of lithium cells with $LiFePO_4$ and $LiFePO_4$-C composite, which were recorded in the second cycle at a scanning rate of 0.02 V s^{-1}.

of only 110 mAh g^{-1} at room temperature (22 °C). As the temperature rose to 40 °C, however, the capacity increased to 156 mAh g^{-1}. This value was very close to the full capacity, as achieved at 50 and 60 °C, respectively. From room temperature to 60 °C, the cell had very similar flat voltage of ~3.4 V although its capacity was significantly different. This is because the temperature mostly affects the diffusion kinetics of Li^+ ions within $LiFePO_4$ grain, instead of the electric polarization relating to the ionic conductivity of electrolyte.

Discharging curves of the Li/$LiFePO_4$-C cell at different current rates are plotted in Fig. 12, which indicates that the capacity is strongly affected by the discharge current, especially in the low current range. At 0.02 C, the capacity achieved 159 mAh g^{-1}, which is close to the theoretical capacity (170 mAh g^{-1}) of the $LiFePO_4$ cathode. However, the capacity rapidly decreased to 143 and 127 mAh g^{-1}, respectively, as the current rate increased to 0.05 and 0.1 C. The strong rate effect can be related to the large size of cathode particles prepared by solid-state reaction.

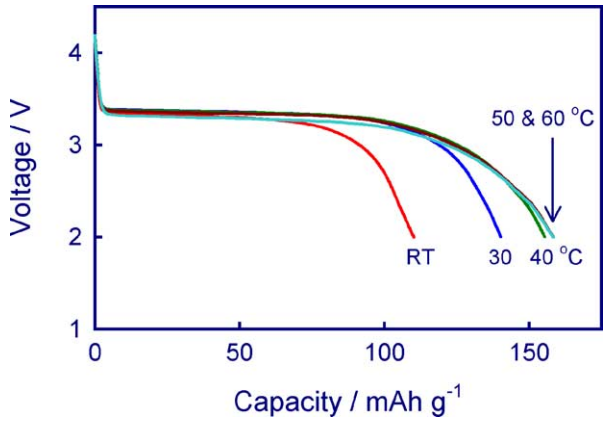

Fig. 11. Discharging curves of the Li/$LiFePO_4$-C cell at different temperatures, which were recorded at 0.5 C. Note that the cell was charged at 0.5 C to 4.2 V and held at 4.2 V until the current declined to 0.05 C.

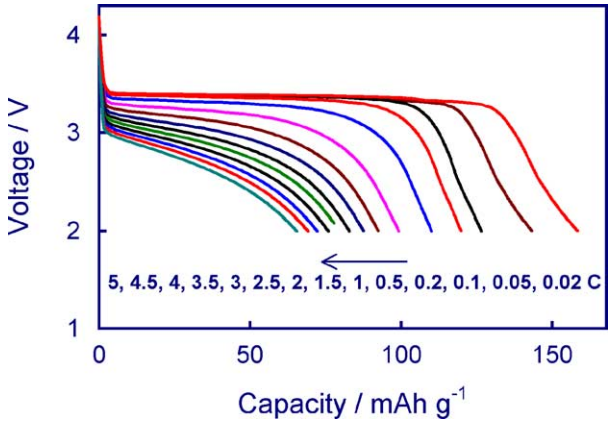

Fig. 12. Discharging curves of the Li/$LiFePO_4$-C cell at different currents, which were measured at room temperature (22 °C). Note that numbers in graph show C-rate of the discharge. Except for the cycling at 0.02 and 0.05 C, in which charge and discharge used the same current, the cell was charged at 0.5 C to 4.2 V and held at 4.2 V until the current declined to 0.05 C.

Fig. 13 compares cycling performance of lithium cells with different $LiFePO_4$ cathodes. In general, the capacity of all these cells was slightly increased in the initial few cycles. Similar phenomena were also reported previously [6,8,13,26,30,31]. We consider that such phenomena are in relation to the self-doping of Li^+ ions into Fe site during the initial cycles. It was noticed that coulombic efficiency of the Li/$LiFePO_4$ cells in initial cycles was less than 100%. This initial irreversibility could be partially attributed to the self-doping of Li^+ ions into Fe sites. It has been reported that self-doping of Li^+ ions in the olivine $LiFePO_4$ takes place during synthesis by the hydrothermal process [33]. Allen et al. [19] intentionally synthesized Li^+-doped $LiFePO_4$ and found it had a much higher conductivity than the pure analog. The initial doping of Li^+ ions into Fe sites greatly increased electric conductivity of the bulk of $LiFePO_4$ cathode, which as

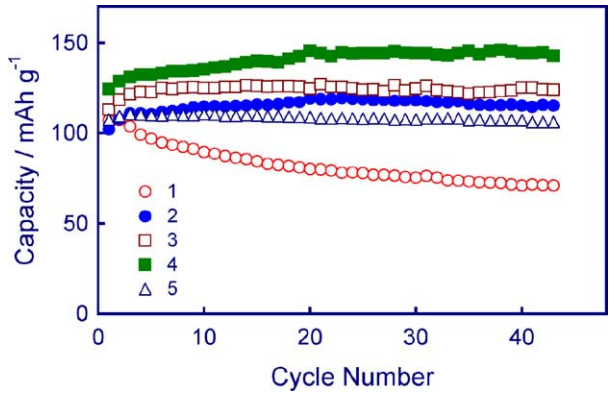

Fig. 13. Cycling performance of lithium cells with different $LiFePO_4$ cathodes. (1) $LiFePO_4$, (2) composite with carbon black, (3) composite with XE 2, (4) composite with black pearls 2000, and (5) composite with graphite SFG6. All composites contained 5% carbon. The cells were cycled at room temperature (22 °C) by charging at 0.2 C to 4.2 V and holding them at 4.2 V for 10 h or until the current declined to 0.05 C, and discharging at 0.2 C to 2.0 V.

a result enhanced the capacity. On the other hand, Fig. 13 indicates that all the cells with $LiFePO_4$-C cathodes exhibited much more stable capacity with increasing cycle number than the $LiFePO_4$ control cell. The cell with black pearls 2000 composite as the cathode achieved a stable capacity of 145 mAh g^{-1}, and those with other composites achieved a stable capacity of 110–130 mAh g^{-1}. It is obvious that the $LiFePO_4$-C composites are superior in the capacity and cycling stability to the pure $LiFePO_4$ cathode.

4. Conclusions

In conclusion, the optimized condition for solid-state synthesis of $LiFePO_4$-C composites is a two-step heating procedure under N_2 flow. The first step is to form a precursor by heating a mixture of carbon and starting materials at 380 °C, and the second step is to form a crystalline phase $LiFePO_4$ by regrinding, pelletizing, and heating the precursor at 800 °C for 5 h. It was found that the appropriate content of carbon in the composites is 3–10 wt.%, and that use of carbon with high specific surface area favors increasing capacity. The composite shows much better performance in terms of the discharge capacity and cycling stability than $LiFePO_4$ alone. However, the capacity of the composite still is very sensitive to the temperature and current rate, which can be attributed to the large size of the composite particles prepared by the solid-state reaction. At room temperature, a stable capacity of 159 mAh g^{-1} at 0.02 C and 145 mAh g^{-1} at 0.2 C, respectively, was obtained from the composite made with 5 wt.% black pearls 2000.

Acknowledgments

The authors would like to thank Dr. J. Wolfenstine for his technical assistance in XRD measurements and valuable discussion on structure characterization.

References

[1] A.K. Padhi, K.S. Nanjundaswamy, C. Masquelier, S. Okada, J.B. Goodenough, J. Electrochem. Soc. 144 (1997) 1609.
[2] D.D. MacNeil, Z. Lu, Z. Chen, J.R. Dahn, J. Power Sources 108 (2002) 8.
[3] M. Takahashi, S.I. Tobishima, K. Takei, Y. Sakurai, Solid State Ionics 148 (2002) 283.
[4] A.S. Andersson, J.O. Thomas, B. Kalska, L. Haggstrom, Electrochem. Solid State Lett. 3 (2000) 66.
[5] A.S. Andersson, J.O. Thomas, J. Power Sources 97/98 (2001) 498.
[6] P.P. Prosini, D. Zane, M. Pasquali, Electrochim. Acta 46 (2001) 3517.
[7] N. Raver, Y. Chouinard, J.E. Magnan, S. Besner, M. Gauthier, M. Armand, J. Power Sources 97/98 (2001) 503.
[8] H. Huang, S.C. Yin, L.F. Nazar, Electrochem. Solid State Lett. 4 (2001) A170.
[9] Z. Chen, J.R. Dahn, J. Electrochem. Soc. 149 (2002) A1184.
[10] M. Herstedt, M. Stjerndahl, A. Nyten, T. Gustafsson, H. Rensmo, H. Siegbahn, N. Ravet, M. Armand, J.O. Thomas, K. Edstroma, Electrochem. Solid State Lett. 6 (2003) A202.
[11] M.M. Doeff, Y. Hu, F. McLarnon, R. Kostecki, Electrochem. Solid State Lett. 6 (2003) A207.
[12] E.M. Bauer, C. Bellitto, M. Pasquali, P.P. Prosini, G. Righinia, Electrochem. Solid State Lett. 7 (2004) A85.
[13] H.T. Chung, S.K. Jang, H.W. Ryu, K.B. Shim, Solid State Commun. 131 (2004) 549.
[14] S.T. Myung, S. Komaba, N. Hirosaki, H. Yashiro, N. Kumagai, Electrochim. Acta 49 (2004) 4213.
[15] Y. Hu, M.M. Doeff, R. Kostecki, R. Finones, J. Electrochem. Soc. 151 (2004) A1279.
[16] F. Croce, A. D'Epifanio, J. Hassoun, A. Deptula, T. Olczac, B. Scrosati, Electrochem. Solid State Lett. 5 (2002) A47.
[17] K.S. Park, J.T. Son, H.T. Chung, S.J. Kim, C.H. Lee, K.T. Kang, H.G. Kim, Solid State Commun. 129 (2004) 311.
[18] S.Y. Chung, J.T. Bloking, Y.M. Chiang, Nat. Mater. 1 (2002) 123.
[19] J. Allen, K. Xu, S.S. Zhang, M. Ding, T.R. Jow, in: 204th ECS Meeting Abstracts, No. 347, Orlando, FL, October 12–17, 2003.
[20] S. Shi, L. Liu, C. Ouyang, D.S. Wang, Z. Wang, L. Chen, X. Huang, Phys. Rev. B 68 (2003) 195108.
[21] S. Yang, P.Y. Zavalij, M.S. Whittingham, Electrochem. Commun. 3 (2001) 505.
[22] P.P. Prosini, M. Carewska, S. Scaccia, P. Wisniewski, M. Pasquali, Electrochim. Acta 48 (2003) 4205.
[23] A. Singhal, G. Skandan, G. Amatucci, F. Badway, N. Ye, A. Manthiram, H. Ye, J.J. Xu, J. Power Sources 129 (2004) 38.
[24] S. Scacciaa, M. Carewskaa, P. Wisniewskib, P.P. Prosinia, Mater. Res. Bull. 38 (2003) 1155.
[25] G. Arnold, J. Garche, R. Hemmer, S. Strobele, C. Vogler, M. Wohlfahrt-Mehrens, J. Power Sources 119–121 (2003) 247.
[26] H.T. Chung, J. Power Sources 133 (2004) 272.
[27] A. Yamada, S.C. Chung, K. Hinokuma, J. Electrochem. Soc. 148 (2001) A224.
[28] H.S. Kim, B.W. Cho, W. Cho, J. Power Sources 132 (2004) 235.
[29] Z.P. Guo, H. Liu, S. Bewlay, H.K. Liu, S.X. Dou, J. New Mater. Electrochem. Syst. 6 (2003) 259.
[30] S. Franger, F.L. Cras, C. Bourbon, H. Rouault, J. Power Sources 119–121 (2003) 252.
[31] S.J. Kwon, C.W. Kim, W.T. Jeong, K.S. Lee, J. Power Sources 137 (2004) 93.
[32] A. Albane, M. Mathieu, W. Calin, G. Sylvain, M. Christian, World Patent WO 2004/001881 A2 (2003).
[33] S. Yang, Y. Song, K. Ngala, P.Y. Zavalij, M.S. Whittingham, J. Power Sources 119–121 (2003) 239.